

DOUBLE-DRIFT BUNCHER*

C. Robert Emigh
University of California, Los Alamos Scientific Laboratory
Los Alamos, New Mexico

Introduction

The more popular theoretical approach to bunching a proton beam for acceptance into a linac has been the harmonic buncher.¹ Depending on the number of harmonics used, this buncher is capable of putting 80 to 95% of the beam current from the injector into the acceptance bucket of the linac. For a high-intensity machine, however, beam loss within the linac at the higher energies is more important than the capture efficiency. A proposed buncher to reduce beam loss, perhaps significantly, is the double-drift buncher first suggested by Ohnuma² as early as 1963. A compendium of the results of our studies over the past few years on the double-drift buncher is presented herein.

Theory, Without Space Charge

The basic operation of the double-drift buncher can be explained with the aid of Fig. 1. Two rf acceleration gaps are separated by the drift distance d_1 . The linac is separated from the second gap by a second drift distance d_2 . A continuous beam of particles of velocity v_0 are velocity-modulated by the first gap according to the sine wave excitation of peak field strength ΔV_1 and frequency w_1 . The modulated beam is allowed to drift to the second gap where it is further modulated according to the field strength ΔV_2 and frequency w_2 . The beam then drifts to the linac and arrives bunched in phase.

The velocity of a particle through the first drift distance is

$$v_1 = v_0 \left[1 + \frac{\Delta V_1}{V_0} \sin(w_1 t_0) \right]^{\frac{1}{2}}$$

where t_0 is the time of arrival of the particle at the first gap. The velocity of a particle through the second drift distance is

$$v_2 = v_0 \left[1 + \frac{\Delta V_1}{V_0} \sin(w_1 t_0) + \frac{\Delta V_2}{V_0} \sin(w_2 \{t_0 + \psi + t_1\}) \right]^{\frac{1}{2}}$$

where t_1 is the time it takes to travel from the first gap to the second gap. The constant ψ is included to allow a phase adjustment between the cavity fields. V_0 is the initial energy in volts.

Using the above equations and the drift distances d_1 and d_2 , the drift times can be approximated closely by

$$t_1 \cong \frac{d_1}{v_0} \left[1 - \frac{\Delta V_1}{2V_0} \sin w_1 t_0 \right]$$

$$\text{and } t_2 \cong \frac{d_2}{v_0} \left[1 - \frac{\Delta V_1}{2V_0} \sin w_1 t_0 - \frac{\Delta V_2}{2V_0} \sin \left(w_2 \left\{ t_0 + \psi + \frac{d_1}{v_0} - \frac{d_1 \Delta V_1}{2V_0 v_0} \sin w_1 t_0 \right\} \right) \right].$$

The time of arrival at the linac, t_L , is calculated from the above times as a function of the time of arrival at the first gap, t_0 :

$$t_L \cong t_0 + \frac{D}{v_0} \left[1 - \frac{\Delta V_1}{2V_0} \sin w_1 t_0 - \frac{(D-d_1)\Delta V_2}{v_0 2V_0} \sin \left[w_2 \left(t_0 + \psi + \frac{d_1}{v_0} - \frac{d_1 \Delta V_1}{2V_0 v_0} \sin w_1 t_0 \right) \right] \right].$$

The synchronous particle is defined as that particle that will go through the entire system at the velocity v_0 ; thus ψ , the relative phase of the second gap to the first gap, is adjusted to $-d_1/v_0$. Under these conditions, $w_1 t_0 = 0, \pi, 2\pi, \text{etc.}$, describe the arrival of the synchronous particle at the first accelerating gap. For a synchronous particle to exist, it is obvious that w_2 must be a harmonic of w_1 .

The phase density of the particles as they arrive at the linac can be related to the inverse of (dt_L/dt_0) . Two regions in phase are of general interest: when $w_1 t_0 = 0, 2\pi, 4\pi, \text{etc.}$, representing the synchronous particle about which the bunch will form; and when $w_1 t_0 = \pi, 3\pi, 5\pi, \text{etc.}$, representing the complimentary phase about which one ideally wants very few particles. Unfortunately, the area of greatest interest ($w_1 t_0 = 0, 2\pi, 4\pi, \text{etc.}$) is usually cluttered by many oscillations of the t_L vs t_0 function, making an optimizing analysis very difficult. However, the region $w_1 t_0 = \pi, 3\pi, 5\pi, \text{etc.}$, will usually have only one value. Thus, optimizing this later region for minimum phase density will more or less establish the approximate conditions for maximum phase density at the complimentary region. By varying d_1 and holding all other parameters constant as demanded by operating characteristics of the linac, one can optimize the bunching. From

$$\frac{d}{dd_1} \left[\frac{dt_L}{dt_0} \right]_{t_0 = \pi/w_1} = 0$$

*Work performed under the auspices of the U. S. Atomic Energy Commission.

we find that
$$d_1 = \frac{D}{2} - \frac{v_0 V_0}{w_1 \Delta V_1}$$

and is independent of both ΔV_2 and w_2 .

Using a practical set of values for these parameters: $D = 310$ cm, $v_0 = 12 \times 10^8$ cm/sec, $V_0 = 7.5 \times 10^2$ kV, $\Delta V_1 = 10$ kV, and $w_1 = 4 \times 10^8$ c/sec; one finds that $d_1 = 83$ cm or about 25% of the total distance D . A more systematic search of the region around 80 cm was made using PARMILA code,³ which was easily adaptable to our problem. The maximum density criteria was confirmed to be near 80 cm; however, the search was far more rewarding in an unexpected direction. A set of parameters was found which gave an exceptionally compact bunch. The phase-energy characteristics of this buncher is shown in Fig. 2 by the dashed line. A typical two-gap harmonic buncher is also plotted for comparison.

The importance of this double-drift buncher is the compactness of the bunch, 76% of the particles being bunched in a phase difference of only 10° . This compares with the harmonic buncher which collects 79% of the beam into a phase difference of 46° . However, caution must be exercised if one is to take advantage of this extremely compact bunch. First, the stability of the Cockcroft-Walton preinjector supply must be improved to reduce the jitter in phase of this bunch. For example, the usual $\pm 0.1\%$ tolerance on the beam energy implies a $\pm 15^\circ$ phase shift. However, C-W stabilities under pulse operation of $\pm 0.05\%$ ($\pm 7^\circ$ phase shift) is common. It would seem that with some effort one could possibly reduce this tolerance to $\pm 0.02\%$ ($\pm 3^\circ$ phase shift). There is no need to try to decrease this tolerance further, because the space charge effects of the beam at 75 mA will cause an energy spread from the outside edge of the beam to its axis, which is comparable to approximately $\pm 0.01\%$ of the beam energy (75 V). Thus, the ultimate total phase spread would appear to be somewhere between 12 and 20° for this double-drift buncher, still a factor of three better in compaction than the harmonic buncher.

If the linac was operated with the admittance bucket as shown in Fig. 2 (synchronous phase angle of -26°), the beam phase density in the regions A and B would determine the high-energy beam loss and, consequently, the radiation problem. In region A, the particle density for the double-drift bunch is 0.069% per degree of phase, whereas the two-harmonic buncher has a density of 0.093% per degree of phase, showing an advantage of the double-drift buncher. However, the compact bunch does open up the possibility of cutting off the tail of the bunch by forming a very tight admittance bucket (small synchronous phase angle) for the first 5-MeV section of the linac, and then opening up the admittance bucket for the rest of the linac. In this manner, it might be possible to force the beam loss to be primarily in the first 5 MeV of acceleration where the radiation problem is not so serious.

The double-drift buncher is practically insensitive to small errors in drift distance,

relative phase, and relative gap field strengths. For practical purposes, distance should be held to 1%, relative phase held to $\frac{1}{2}^\circ$, and field strengths to 1%.

Space Charge

To analyze the action of the double-drift buncher with the effects of space charge included, one must resort to atomistic methods that treat the beam as a population of small elements. Depending on the nature of these elements, one can at least approximate the space-charge force between these elements and write differential equations of motion for their coordinates. These equations can then be integrated numerically, and fairly accurate results can be interpreted from the integrated coordinate values. A number of different approaches to this problem were tried -- many discs, many circular rings, and many elliptical rings. However, the greatest success was from a program called Many Rings Averaged (MRA),⁴ which is capable of including solenoidal lenses and transient time corrections for the cavities.

In MRA, the r-z space of a beam of particles is covered with a rectangular mesh. At any given time, the number of particles contained within a given rectangular box is considered to act as a ring of charge located at the centroid of that box. The r and z components of the space-charge electric fields are then computed at all the mesh points. The electric field felt by each particle is obtained by a linear interpolation consistent with the particle's position with respect to the mesh points. The program computes the positions of the particles as the beam goes through one or two bunchers and an ideal focusing lens. The rectangular mesh covers a section of the beam that is one wavelength of the first buncher frequency in length. The beam is assumed to be periodic in the z direction and the effects of neighboring sections is taken into account when computing the electric fields at the mesh points.

Figures 3a through 3h were produced by MRA for a typical case; they show the condition of the bunch at various times. In this particular case the beam current was 20 mA, the initial radius was 0.7 cm, and the effective voltages on the two buncher cavities were $V_1 = 20$ kV and $V_2 = -13$ kV, respectively. The first buncher cavity operates at a frequency of 200 MHz, whereas the second operates at 400 MHz. The positions of the buncher cavities and focusing lens are shown at the top of each figure. The tiny rectangle represents the position of the beam bunch. In the middle of each figure is shown the distribution of the rings in r-z space. The distributions in the longitudinal and transverse phase spaces are shown at the lower left and lower right, respectively. The uniformly charged beam entered the first buncher at a waist and with zero emittances in both the longitudinal and transverse phase spaces. As well as bunching the beam, the buncher cavities focus and defocus different parts of the beam, producing a spread in the transverse phase space. In Fig. 1h, approximately 88% of the particles in the section have been bunched to lie within a phase angle of

$\pm 30^\circ$. The transverse emittance of the beam has been increased 1 cm-mrad.

Ignoring space-charge effects, it is possible to obtain a set of optimum parameters for a buncher system; that is, a set of buncher voltages and drift distances that will cause the largest percentage of particles to be bunched within a specified phase angle. The three curves of Fig. 4 show the maximum percentage of particles (not including space charge) that could be expected to be bunched within a range of phase angles for three different types of buncher systems: (1) a double-drift buncher (top curve), in which there are two buncher cavities separated by a drift distance and the second cavity, operating at twice the frequency of the first; (2) a harmonic buncher (middle curve), in which there is no drift distance between the two cavities; and (3) a simple buncher (bottom curve), in which there is only one cavity.

It is of interest to compare these curves with some points obtained by MRA for three different currents. In all cases, the initial radius of the beam was 0.7 cm, the voltage of the first buncher was 20 kV, and the final bunched beam radius was required to be 0.7 cm. The MRA program was searched for optimum parameters to maximize the percentage of particles within a given phase spread. These points are indicated on Figs. 5, 6, and 7. In general, the points can be brought closer to the zero-current curve by increasing the first cavity buncher voltage. In practice, however, this will be limited by the acceptance of the linac.

Some general observations can be made in regard to the design of the double-drift buncher. Higher buncher voltages reduce space-charge effects but increase the spread in the transverse phase space, unless grids are placed on the buncher cavities to remove the focusing-defocusing effects. To obtain optimum bunching with a double-drift buncher as the current increases, the distance between the two buncher cavities must be decreased and the magnitude of the second buncher voltage must also be decreased. The double-drift buncher can also be operated with the second cavity frequency the same as that of the first cavity. In this case, there may not be a synchronous particle. The compaction of the beam will probably be somewhat less in this case; however, it may be a much more practical buncher to build.

Acknowledgments

I would like to acknowledge the contributions of Alan Hindmarsh, a 1966 summer graduate student with the Los Alamos Scientific Laboratory, for his theoretical work in writing many different computer programs in an effort to find a satisfactory one. Although his work has since been pre-empted by an improved approach, it was of great value in the later generation of the more accurate program.

I would especially like to thank Kenneth Crandall for his theoretical work in developing the MRA program, for his computer searches to determine optimum operating conditions for the

double-drift buncher, and for many fruitful discussions concerning the display of information.

References

1. R. Perry, Minutes of the Conference on Proton Linear Accelerators, Yale, October 1963, p279.
2. S. Ohnuma, Minutes of the Conference on Proton Linear Accelerators, Yale, October 1963, p273.
3. D. A. Swenson, 1964 Linear Accelerator Conference, MURA, July 1964, p328.
4. K. R. Crandall, "MRA, a FORTRAN IV Code to Simulate Beam Bunching," MP Internal Report MP-4/KC-3, March 1967.

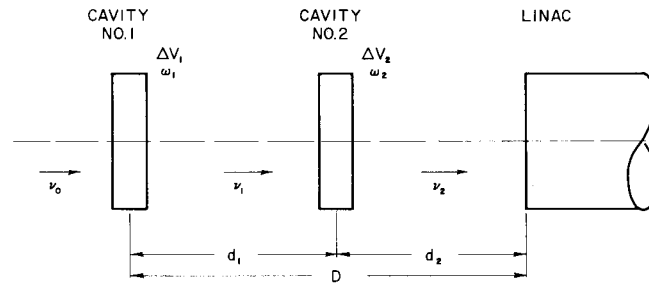


Fig. 1. Schematic layout of the double-drift buncher.

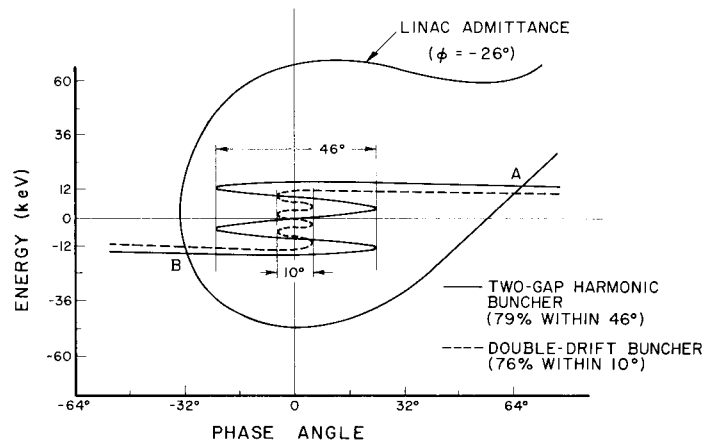


Fig. 2. Phase-energy particle distribution at linac entrance.

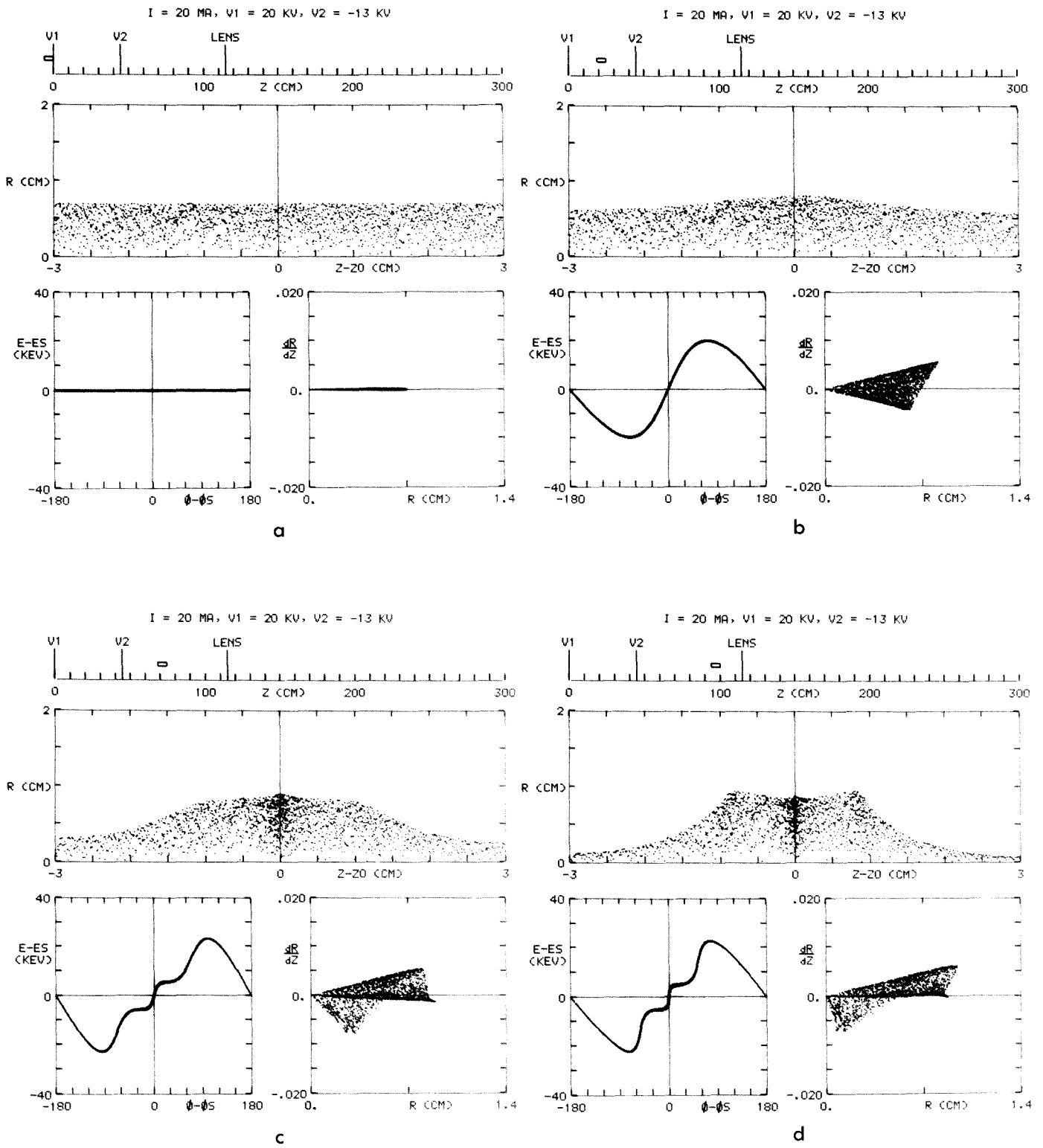
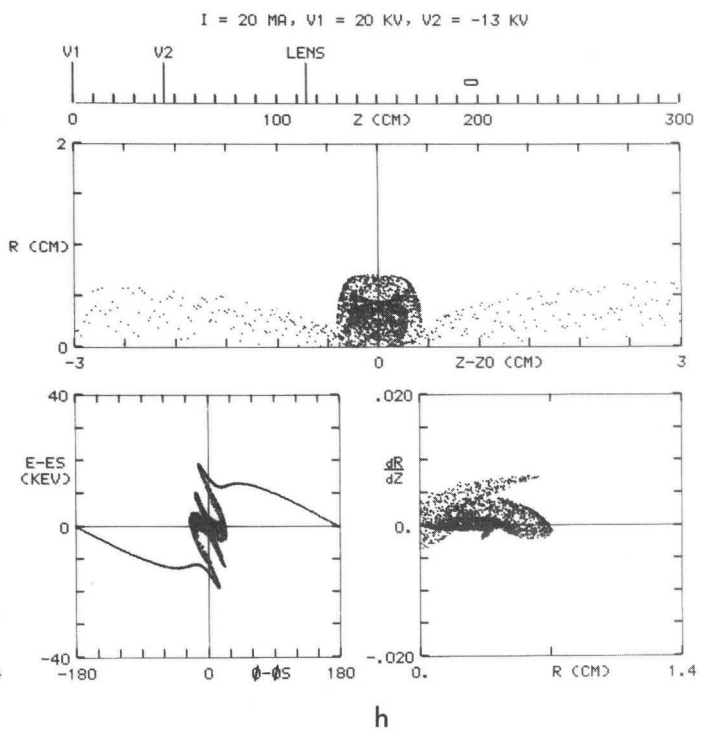
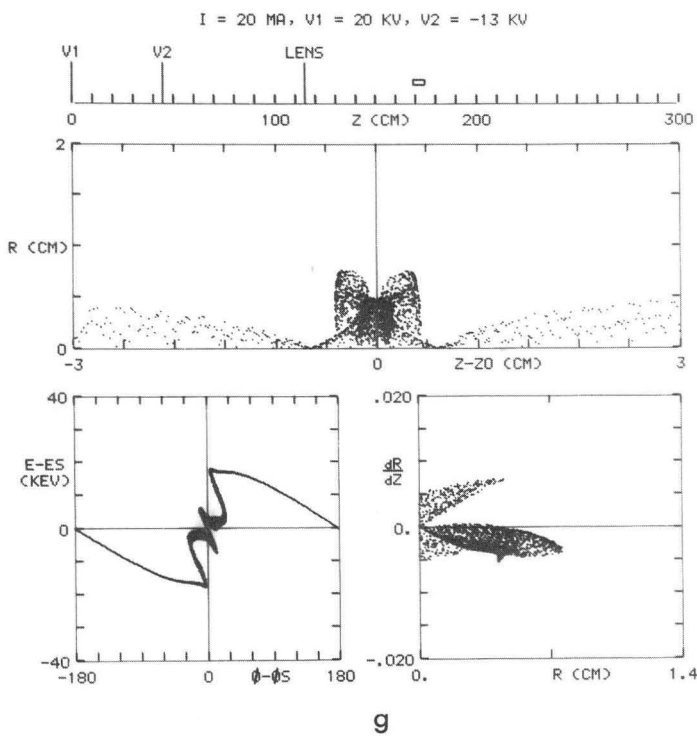
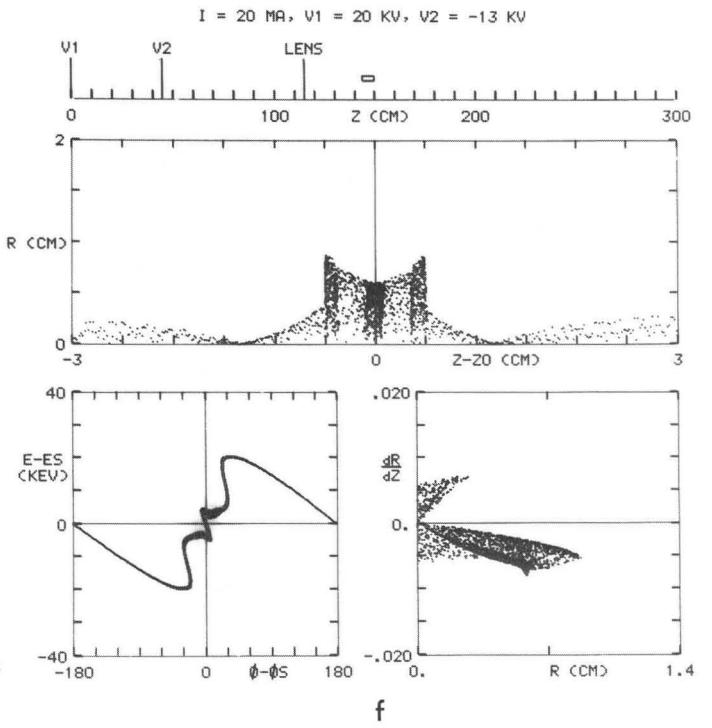
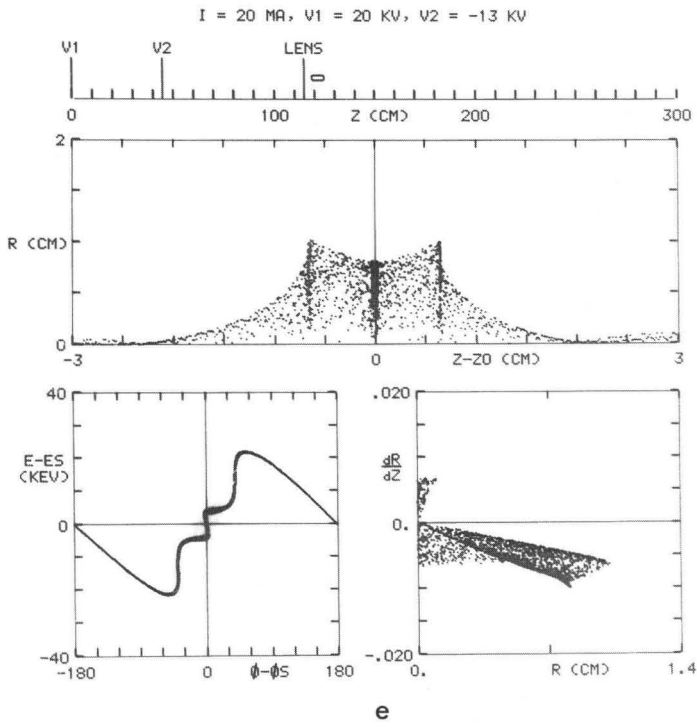


Fig. 3. (a-h) MRA Phase plots of particles as a function of bunch position along the axis of the double-drift buncher.



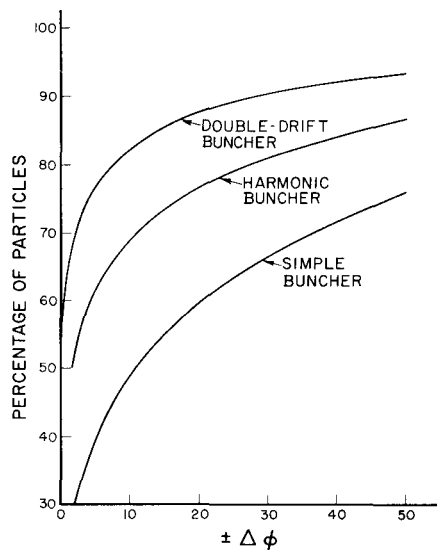


Fig. 4. Maximum percentage of particles that can be bunched within a phase of $\pm\Delta\phi$ for various types of bunchers, space charge neglected.

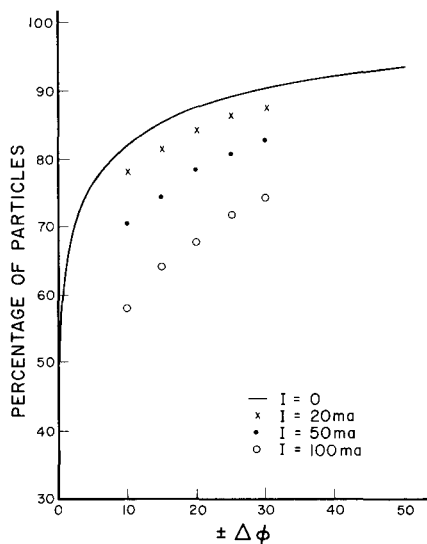


Fig. 5. Comparison of space-charge effects on the maximum percentage of particles that can be bunched within a phase of $\pm\Delta\phi$ and for a voltage of 20 kV on the first cavity, using a double-drift buncher.

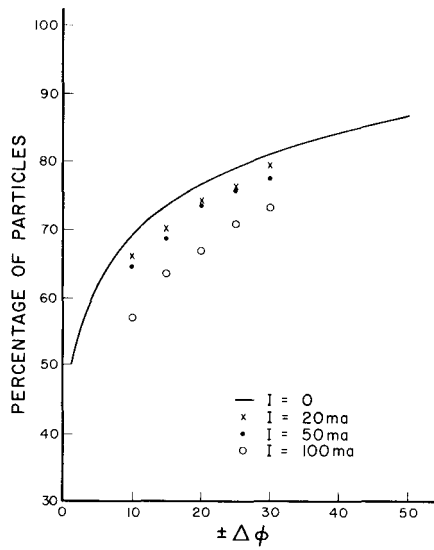


Fig. 6. Comparison of space-charge effects on the maximum percentage of particles that can be bunched within a phase of $\pm \Delta \phi$ and for a voltage of 20 kV on the first cavity, using a two-gap harmonic buncher.

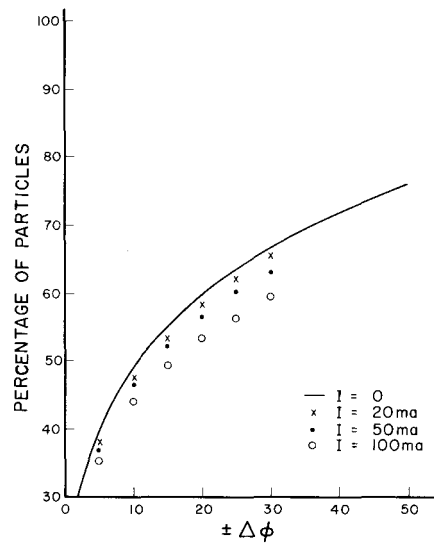


Fig. 7. Comparison of space-charge effects on the maximum percentage of particles that can be bunched within a phase of $\pm \Delta \phi$ and for a voltage of 20 kV on the cavity, using a single-cavity buncher.